Environmental Science & Technology

pubs.acs.org/est

Article

Seasonal Landfill Methane Emissions Driven by Temperature and Pressure

Andrew Hallward-Driemeier,* Yuwei Zhao, Matthew Drews, Maryann Sargent, Steven Wofsy, Rory Barton-Grimley, Ashwin Yerasi, James Collins, Amin Nehrir, and Róisín Commane

Cite This: https://doi.org/10.1021/acs.est.5c16757

Read Online

ACCESS | Metrics & More | Article Recommendations | Supporting Information

ABSTRACT: More than a quarter of anthropogenic global warming has been attributed to methane growth in the atmosphere. Landfills account for 17% of estimated methane emissions in the United States of America (USA), according to the Environmental Protection Agency (EPA), but studies show that many landfills emit more than reported. We developed a novel method to calculate monthly methane emissions from an active landfill using atmospheric methane mixing ratios observed from a single tower in New Jersey, USA. The tower method provides two and a half years of semicontinuous measurements and therefore observes more of the variability of methane emissions and lacks the sampling bias present in other methods. Time-specific comparison of tower-based methane emissions against those observed from summertime aircraft sampling and year-round mobile ground-based platforms showed good agreement. Estimated methane emissions for 2023 were five times greater than those reported to the EPA. We observed a strong seasonality in methane emissions, with a peak in the winter and a minimum in the summer. This seasonal cycle was driven by a strong negative dependence on air temperature and the change in atmospheric pressure. Our results highlight the importance of observations in nonideal weather conditions (such as declining pressure and near-freezing temperatures) when methane emissions are largest. We suggest that this methodology could be applied to other suitable landfills to improve estimates of methane emissions.

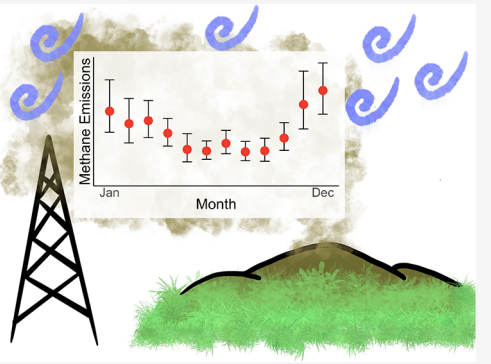

KEYWORDS: *greenhouse gas, methane, landfill, solid waste*

INTRODUCTION

Methane (CH_4) is the second most important anthropogenic greenhouse gas, behind carbon dioxide (CO_2), with a global warming potential 80 times that of CO_2 over 20 years.[1] CH_4 has contributed 26% of global warming since the 1850s.[2] The largest source of methane globally is from freshwater wetlands, with anthropogenic sources such as fossil fuels, agriculture, and waste also emitting at least 10% of global methane emissions each.[3] The Environmental Protection Agency (EPA) estimates that landfills emit 17% of total methane emissions in the United States of America (USA),[4] but several studies indicate that this percentage may be an underestimate.[5−9] Landfill methane emissions reported to the EPA Greenhouse Gas Reporting Program (GHGRP) have decreased by 40% since 1990, with this reduction attributed to the adoption of gas capture technology and better management.[4] However, satellite observations since 2010 have not observed this reported decline.[5] Instead, these studies have suggested that much of the decline may reflect changes in the methodology used to calculate methane emissions; from a method based on the amount of waste-in-place to a method based on the amount of gas captured, assuming a constant capture rate.[10]

Within landfills, methanogenic archaea break down organic waste, producing methane that is either consumed by methanotrophs in the soil cover, extracted by gas capture systems, or emitted into the atmosphere. The rate of production of methane peaks at internal temperatures of about 30 °C.[11] The emission of landfill gas into the atmosphere is subject to both subdaily and seasonal variability. Methane emissions can range over 2 orders of magnitude within a day, where emissions increase due to faster wind speeds,[12] lower atmospheric pressures,[13−20] and optimal soil moisture.[13,21,22] On a seasonal scale, methane emissions through the surface soil decrease with soil oxidation rates[23−25] that peak at warmer soil temperatures,[26−29] and increase with the frequency of low-pressure systems.[14,20,25,30]

To mitigate the emission of untreated landfill gas into the atmosphere, large landfills employ gas capture systems on capped cells within the landfill. These systems extract landfill gas from the interior of the landfill to a collection point where the methane is burned. They also use cap landfills with soils

Received: November 24, 2025
Revised: April 23, 2026
Accepted: April 24, 2026

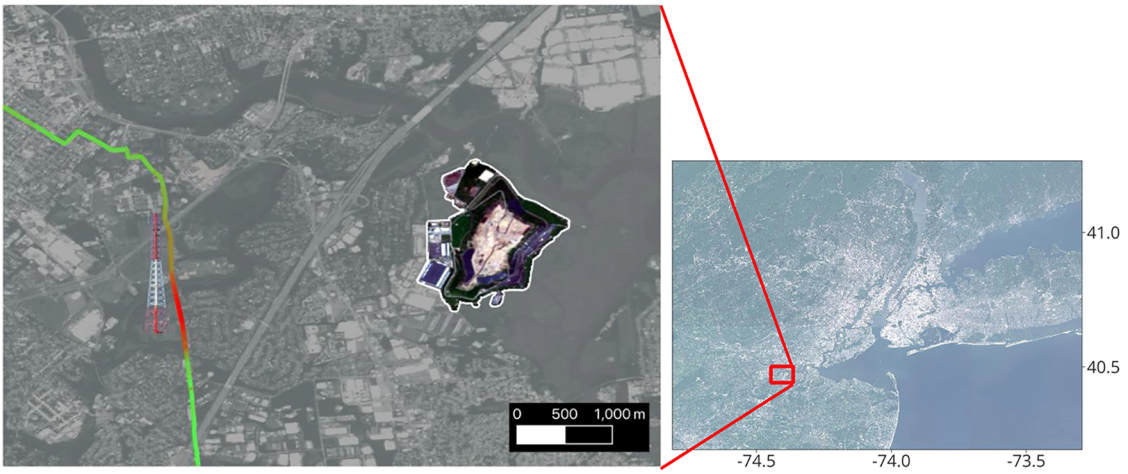

Figure 1. Map of the area surrounding the Middlesex County landfill complex in northern New Jersey, with the area of the landfill highlighted in white and the approximate site of the open face in orange. Approximate location of the tower is shown, as is the routes of three example mobile transects, colored by the methane enhancement (background in green, high enhancements in red). Imagery from Copernicus Sentinel data [2025]. Retrieved from Copernicus SciHub [3 September 2025], processed by ESA.[58]

that encourage the growth of methanotrophs. Active landfills cannot use gas capture systems over the open face while it accumulates waste, and only cover the waste each day with a thin layer of daily cover. As a result, open faces of landfills (and, to a lesser extent, intermediate cover areas) typically emit far more methane than closed areas of landfills.[8,31−33]

Methods for estimating methane emissions from landfills vary widely. Two methods (EPA Method 21 and OTM 51), which are often required by the EPA to identify leaks, entails walking or flying a drone around the landfill with a detector to identify hot spots of methane emission, but do not quantify whole-landfill emissions.[34] Other methods used in research include field chambers,[23,24,35,36] fence-line analyzers,[37−39] long-path spectrometers,[31,40,41] tracer−tracer correlations,[40,42,43] spectral-imaging drones,[33,44] vehicle measurements,[29,45] flights,[8,39,46,47] or satellites.[6,7,39,48−50] One important difference between these methods is the distance from the emission source.

On-site methods are best suited for source identification and location, while off-site methods perform best at quantifying whole-landfill emissions. On-site methods, due to their proximity to the sources, provide much higher resolution spatial information that can easily identify leaks or other issues. However, these methods typically struggle to quantify methane emissions due to high variability in methane concentrations from small-scale wind eddies or emission hot spots.[12,51,52] On-site methods may also give incomplete results, as they typically require extrapolating results from the sampled section to the entire landfill and may miss emission hot-spots.[53,54] Many of these methods also have a low sampling frequency as they typically require researchers onsite to perform measurements. Other methods, such as soil chambers and fence-line measurements, can be conducted semicontinuously with infrequent personnel visits for maintenance. Off-site methods capture integrated plumes of methane emissions, thereby observing all emissions from the site and more accurately quantifying emissions. However, these off-site methods have smaller enhancements and typically require much more accurate measurements of methane (and therefore more expensive instruments), are unlikely to identify individual sources within the landfill, and rely on accurate measurement of meteorological parameters. While most of these methods, such as satellites or vehicle measurements, are not continuous, tower-based instruments can sample semicontinuously, depending on the wind direction.

In this study, we combined long-term, high-time resolution tower-based observations of methane mixing ratios with ground-based mobile in situ and airborne remote sensing observations to quantify the methane emissions from an active landfill. We evaluated the various methods used and quantified the uncertainties in the fluxes. We also considered the influence of meteorological drivers on methane emissions and the importance of understanding the seasonality of emissions when interpreting our semicontinuous observations from a single landfill.

METHODOLOGY

Site Description

The landfill complex studied in this paper is located in northern New Jersey (40.4726° N, 74.3870° W). An active landfill, Middlesex County Landfill, started operations in 1992. It has since expanded over the site of Edgeboro landfill, which closed on this site in 1994 but continues to separately report emissions to the EPA. Middlesex County Landfill currently has over 16 million metric tons of waste and accepts another 500,000 t of waste each year. The two landfills have an extensive gas capture system.

Other potential methane sources in the area include two old, smaller, landfills, which closed in the 1970s, that are located to the north of the site but contain mostly industrial waste. These landfills are too small and old to report methane emissions to the EPA. The landfills are also located near a tidal wetland along the Raritan River, a composting facility located two kilometers to the north of the landfill complex, and a wastewater treatment plant approximately six kilometers northeast of the landfill complex. We attempted to quantify methane emissions from the composting facility and wastewater treatment plant through mobile measurements (described below). However, enhancements were small enough that we were only able to quantify upper bounds of 150 and 200 kg/h for the composting and wastewater treatment facilities, respectively. The MethaneAIR flight (described

https://doi.org/10.1021/acs.est.5c16757
Environ. Sci. Technol. XXXX, XXX, XXX−XXX

below) also identified enhancements above the instrumental noise for only the Middlesex landfill complex in this area.

Reported Methane Emissions Estimates

Edgeboro and Middlesex County landfills calculate methane emissions using one of the two methods approved by the EPA GreenHouse Gas Reporting Program (GHGRP). The "captured" method is calculated by measuring the volume of captured landfill gas and assuming a gas capture efficiency determined by the landfill cover characteristics. This methodology requires a gas capture system, which both landfills have. The waste-in-place ("WIP") method estimates methane production from the organic fraction and age of the waste within the landfill and then subtracts off captured methane.

Edgeboro, the closed landfill, reported an estimated methane emission of 26 kg/h using the captured method and 577 kg/h using the WIP method (20 times higher than the captured method) for 2023.[55] Middlesex County reports 510 kg/h for the captured method and 403 kg/h for the WIP method for 2023. Both landfills have chosen to report the estimate based on the captured method to the GHGRP to give a combined emission of 536 kg/h for 2023. Edgeboro switched to the captured method, which has consistently estimated methane emissions much lower than the WIP method, in 2019. Middlesex County has consistently used the captured method, even when it was an order of magnitude larger than the WIP estimate in 2010. The captured method at Middlesex County shows a consistent decreasing trend from 2010 to 2023, while the amount of waste onsite (and therefore the WIP estimate) has continued to increase across this time period.

Observations

Tower Observations. We measured atmospheric dry mole fractions of methane (hereafter referred to as mixing ratios) from the 20 m tower (agl, above ground level) at an EPA Photochemical Assessment Monitoring Station (PAMS) on the campus of Rutgers University in New Brunswick, New Jersey (40.4623° N, 74.4293° W, Figure 1).[56] The closest part of the landfill was 3.3 km to the East and the tallest part of the landfill was 3.85 km away (Figure 1). For the flux calculations below, we have assumed a point source emission 3.85 km away from the tower. The landfill covers wind directions between 65 and 80 degrees, to the east of the tower. However, observed methane enhancements typically centered on the north end of the landfill (where the open face is) so we used 66 degrees as the center point for all calculations. Imaging from the MethaneAIR flight (described below) also indicated methane emissions predominantly from the north end of the landfill. We measured mixing ratios of methane, carbon dioxide (CO_2), carbon monoxide (CO), and water vapor (H_2O) using a Picarro G2401 from January 2023−July 2025. To characterize the sources of methane, we also deployed an Aeris MIRA Ultra Natural Gas analyzer (CH_4 and ethane (C_2H_6)), and an Aeris MIRA Ultra nitrous oxide (N_2O/CO) analyzer (see Supporting Information S1) for May−August 2024. We aggregated the trace gas data to a uniform 10 s temporal resolution during our initial data processing. All reported mixing ratios were corrected for humidity based on testing completed on each instrument prior to deployment following the method in Commane et al.[57]

Two calibration cylinders with mixing ratios above and below ambient mixing ratios for each of the measured gases, were each sampled once per day. These cylinders were calibrated prior to deployment using an Aerodyne SuperDUAL spectrometer and Picarro G2401 using standards calibrated by the Central Calibration Laboratory at the National Oceanic and Atmospheric Administration (NOAA) Global Monitoring Laboratory in Boulder, CO. CCL maintains the World Meteorological Organization (WMO) CH_4 scale (WMO X2004A) and CO_2 scale (WMO X2019).

For each day, we calculated a slope and intercept from the two tank calibration, which we then interpolated and applied to the humidity-corrected 10 s trace gas data. We evaluated other methods of applying the calibration, including a smoothing spline rather than interpolation, and found that the different methods resulted in a less than 1 ppbv methane change at near-ambient mixing ratios. After accounting for analyzer time drift and the observed 9 s delay from the inlet to the analyzer, the mean of the calibrated mixing ratio was calculated for every 30-s period, matching the resolution of the meteorological data collected onsite.

Tower-Based Meteorology. At the landfill complex, the New Jersey Mesonet meteorological network measures wind speed and direction with a R. M. Young Company 05103 Wind Monitor, barometric pressure with a Vaisala PTB110 Barometer, and air temperature with a Campbell Scientific EE181 Thermometer & Hygrometer. We used these measurements to analyze the drivers of methane emissions at the landfill site.

At the PAMS tower, mean wind speed and direction at two heights on the tower (20 and 10 m agl) were reported every 30 s from two Gill Windmaster HS 3-D Sonic Anemometers; temperature and relative humidity were recorded every 5 min on a Campbell Scientific HygroVue 10; pressure was recorded every 5 min from an RM Young 61402 V; and solar irradiance was reported every 30 s using a Kipp & Zonen CMP-22. For times when the temperature and pressure sensors at the PAMS site were offline, we used the equivalent data measured at the landfill site, correcting for differences between the two instruments (see Supporting Information S2). During our analysis, we identified a problem with the logged wind direction that was fixed in February 2025, which reduced the availability of data before the fix was implemented. However, this mainly affected wind directions around due north and had little effect on our results (see Supporting Information S3 for details).

To ensure that the wind direction we used was representative of the larger-scale wind patterns, we calculated the mean 20 m agl wind speed and direction over a variable time window corresponding to the travel time between the landfill and the site rather than the instantaneous wind speed and direction. We only included observations where the estimated mean wind direction at the PAMS site was within 15° different from the observed wind direction at the Mesonet station. Approximately half of the data passed this filter.

Ground-Based Mobile Observations. Over 3 days in 2025 (one in February, two in May), we estimated methane emissions from the landfill complex with the New York Atmospheric composition and Air Quality (NYAAQ) Mobile Laboratory to complement the ongoing tower measurements (Figure 1). The mobile laboratory was instrumented with a LI-COR LI-7810 Trace Gas Analyzer (CH_4, CO_2, and H_2O) logging to the same computer as a GPS receiver. Ambient air was sampled from an inlet mounted on top of the vehicle, 1.8 m above the ground. The analyzer was calibrated within a day of the deployment with tanks on the same calibration scales as the tower measurements. We previously tested the stability of

https://doi.org/10.1021/acs.est.5c16757
Environ. Sci. Technol. XXXX, XXX, XXX−XXX

the calibration when turning the analyzers on and off and found that the uncertainty in the methane mixing ratios around ambient level was about 5 ppbv. We also used an Aeris MIRA Ultra LDS (CH_4, C_2H_6, and H_2O) to identify and remove natural gas-related methane peaks.

One of the days involved driving along the road next to the tower. For the other 2 days, the wind direction and geometry of the roads meant that driving occurred in a different area in order to intercept the landfill plume. When possible, we performed two loops on the same day at different distances from the landfill, which has been shown to improve estimates of the plume dispersion.[40,45,59] For each drive, we focused on repeating downwind measurements and only sampled upwind of the landfill once per day. The methane mixing ratios and variability for the upwind leg were far smaller than those of the downwind legs, making repeating the downwind measurements more important to reducing uncertainty.[60] Most of the driving occurred overnight to minimize the traffic encountered.

Aircraft-Based Observations. Two different airborne measurement techniques were used to sample methane emissions from this landfill complex during our measurement period.

High-Altitude Lidar Observatory (HALO). HALO is a NASA developed multifunction airborne lidar that provides measurements of water vapor and aerosol/cloud profiles or methane columns and aerosol cloud profiles and serves as a simulator for future space-based trace gas lidar missions.[61] For the summer 2023 Synergistic TEMPO Air Quality Science (STAQS) campaign, HALO employed the integrated path differential absorption lidar technique to measure column integrated methane mixing ratio (XCH_4)[62] and the high spectral resolution lidar technique to obtain aerosol/cloud profiles[63] and distributions of mixed layer heights.[64] During the STAQS campaign in July and August 2023,[65] HALO was operated on the NASA Gulfstream-III research aircraft flying at 12 km altitude and measured XCH_4 with <18 ppbv precision at approximately 100−150 m spatial resolution along a narrow track. HALO sampled downwind of the Middlesex Landfill complex on July 26, 2023.

MethaneAIR. MethaneAIR is an infrared imaging spectrometer which uses a CO_2 proxy retrieval to calculate column XCH_4. It is the airborne simulator for the MethaneSAT satellite. It flew on a modified Learjet aircraft at an altitude of 12 km. Unlike the single point measurement of HALO, MethaneAIR has a 4.5 km swath width and produces images at 10 m x 10 m resolution with 17−20 ppbv standard deviation on a flat scene.[66] The instrument's calibration[67,68] and retrieval methods[69] have been previously described. MethaneAIR sampled the area around the Middlesex Landfill complex on September 3, 2023.

Flux Calculation Methods

We calculated the methane flux from the landfill using two methods. We adapted (i) two forms of the Divergence Theorem, also known as the mass balance method, for the aircraft data and (ii) a Gaussian Plume Dispersion method to the observations from the tower and mobile drives.

Divergence Theorem—Mass Balance Method. The two aircraft remote-sensing instruments calculated a methane flux using slightly different forms of the divergence theorem. The divergence theorem is based on the principle that the total flux emitted into or removed from a fixed volume is equal to the sum of the surface integral of fluxes over the sides of the volume. We assumed that the plume did not mix across the top and bottom of the volume and enhancements in the trace gases were measured along the remaining sides. We defined the bottom of the volume as the ground. The aircraft observations used in this study measured the total column of methane, so the height of the volume was the height of the column. We also tested a mass balance method for the tower data, but it did not perform as well as the Gaussian Plume Dispersion method described below (see Supporting Information S4).

High-Altitude Lidar Observatory (HALO). A methane emission rate from the HALO methane column differential optical depth ($Q_{CH_4}^{aircraft}$) was calculated using the plume integration technique[66,70−74] (eq 1 and 2). Meteorological variables, including air temperature, pressure, wind speed and wind direction were subsampled to each lidar footprint from the NOAA HRRR 3-km model.[75] For each location along the plume track, we calculated the product of the mass of methane in the plume times the wind vector

$$P^{CH_4} = \mu^{CH_4} \overline{n}_z \overline{u}_{xy} \tag{1}$$

μ^{CH_4} is the mass of a methane molecule. $\overline{n}_z$ is the column integrated methane number density from the surface up to altitude z, the vertical extent of the plume, which is derived from the HALO observations. The two-dimensional vector $\overline{u}_{xy}$ is the horizontal component of the wind averaged from the ground up to z. This vector is dotted with the unit vector $\hat{m}_i$, which is pointed in the direction normal to the line segment between the two consecutive points. Then the flux is calculated as the sum along the flight track

$$Q_{(CH_4)}^{aircraft} = \frac{1}{2} \sum_{i=1}^{N-1} \Delta l_i [P_i^{CH_4} + P_{(i+1)}^{CH_4}] \cdot \widehat{m_i} \tag{2}$$

The length Δl_i is the physical distance between two consecutive points on the ground (i and $i + 1$). Because HALO measures column XCH_4, the true vertical distribution of the methane in the landfill's plume is unknown and it is therefore uncertain to which exact altitude the wind vector should be averaged. In this study, the two logical extremes are used: the altitude just above the laser spot on the ground surface and the mixing layer height measured by HALO (MLH_{obs}). The ground surface elevation is measured from the HALO's time-of-flight capability while the MLH_{obs} is calculated using gradients in the aerosol measurements derived from the High Spectral Resolution Lidar (HSRL) channels.[64]

MethaneAIR. MethaneAIR used the flux divergence method, which combines principles of the divergence theorem described above for each swath (10 m × 10 m pixel across 4.5 km width) to calculate a methane emission rate.[66] A series of boxes were drawn around the source, with the size of the box growing sequentially in each direction by one MethaneAIR pixel (10 m), and the downwind side of the box extending across the length of the plume. The total landfill flux is estimated by averaging the flux divergence from that set of boxes to calculate the mean methane flux. Because the set of boxes cover multiple eddy scales, the method averages out the impact of local eddies, which are not captured in the large scale HRRR winds. This flux divergence method was validated in blind controlled-release experiments, which showed excellent agreement between the method and known methane emissions ranging from 200−1300 kg/h.[76]

https://doi.org/10.1021/acs.est.5c16757
Environ. Sci. Technol. XXXX, XXX, XXX−XXX

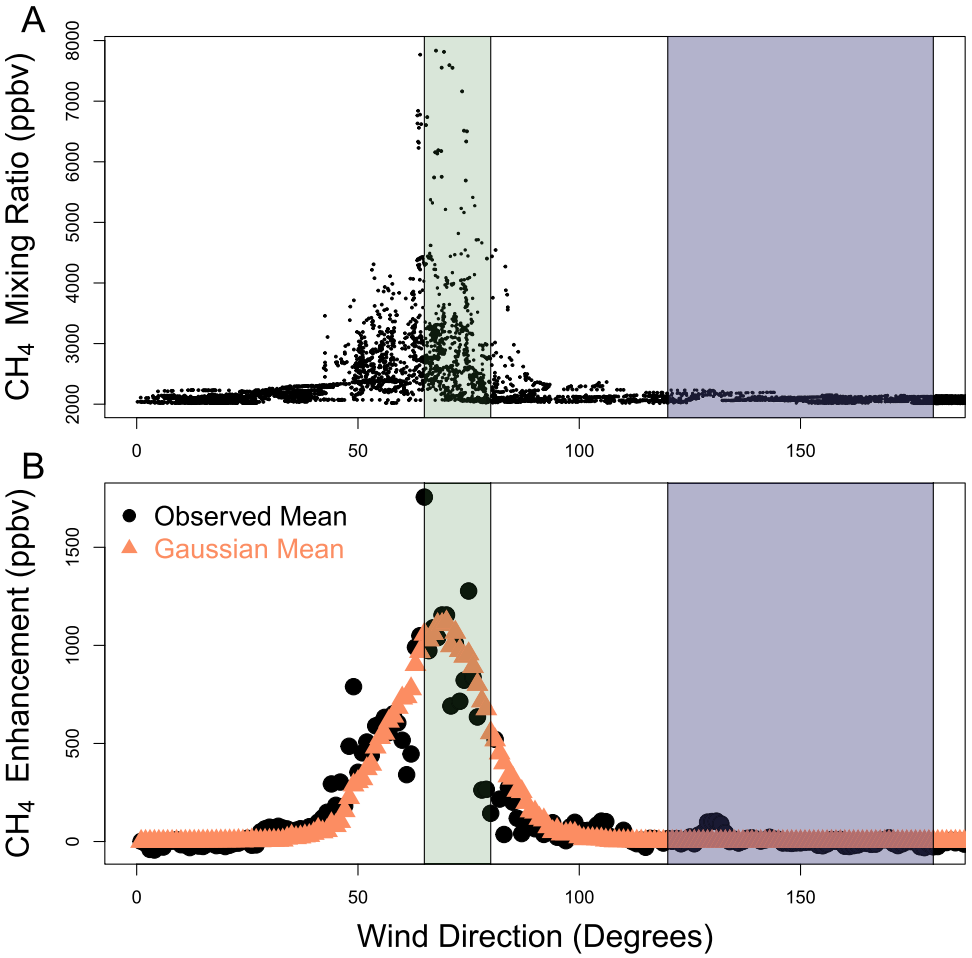

Figure 2. Methodological overview for the stationary tower site showing the Gaussian Plume Dispersion method. (A) shows each 30-s observation, while (B) compares the mean methane enhancement by 1° wind direction bin against the mean from the GPD method. The GPD method estimates the flux using a Monte Carlo draw from the ratio of the observed enhancements to the modeled GPD enhancements using eq 4. The wind directions for the landfill (green; 65−85 degrees) and background (purple; 120−180 deg) are shaded for reference.

Gaussian Plume Dispersion (GPD). The Gaussian Plume Dispersion (GPD) method was used to calculate monthly methane fluxes for the tower and individual drive dates for the mobile measurements. We approximated the dispersion of a gas downwind of its source as Gaussian in the crosswind and vertical directions, with a reflection at the ground. The method estimates the methane enhancement at any given downwind point as

$$\Delta c(x, y, z) = \frac{Q_{CH_4}^{Initial}}{2\pi\sigma_y\sigma_z\overline{u}} \cdot \exp\left(-\frac{y^2}{2\sigma_y^2}\right) \cdot \left[\exp\left(-\frac{(Z-H)^2}{2\sigma_z^2}\right) + \exp\left(-\frac{(Z+H)^2}{2\sigma_z^2}\right)\right] \quad (3)$$

where Δc is the enhancement of methane (in g m^{-3}) observed at a specific location (x = downwind, y = crosswind, z = vertical), $\overline{u}$ is the mean wind speed along the plume, Z is the vertical measurement height (20 m tower or 2 m vehicle), H is the emission height (assumed to be the top of the landfill at 50 m) and σ_z and σ_y are the dispersion parameters represented by the standard deviations of the plume distance in the crosswind and vertical directions and are a function of atmospheric stability (wind speed and insolation).[77] We estimated the sensitivity of the chosen emissions height on the estimated fluxes to be around 5%. We used the GHGRP estimate of 536 kg/h for our initial estimate of the methane emissions $Q_{CH_4}^{Initial}$. Methane enhancements were calculated against a three-day centered running mean of methane mixing ratios in the background wind direction (see Supporting Info S5 for more detail).

We calculated σ_y from the observed enhancements across the plume. For the mobile drives, we estimated σ_y from a Gaussian fit to the observed width of the plume for each individual loop. Using all the stationary tower data, we grouped the observations by insolation and wind speed, averaged over a variable time window corresponding to the transport time from the landfill to the tower, and estimated σ_y from a Gaussian fit of observed enhancements against wind direction by group. We then parametrized a function for σ_y as a function of insolation and wind speed. Here we used a lower-bound estimate of the ratio of $\frac{\sigma_z}{\sigma_y}$ of 0.25, the value for the most stable conditions. For a more detailed sensitivity study of this choice, see Supporting Information S6. This choice had minimal effect on the results of the mobile drive sampling as most of the driving occurred overnight when $\frac{\sigma_z}{\sigma_y}$ is expected to be around 0.25.

https://doi.org/10.1021/acs.est.5c16757
Environ. Sci. Technol. XXXX, XXX, XXX−XXX

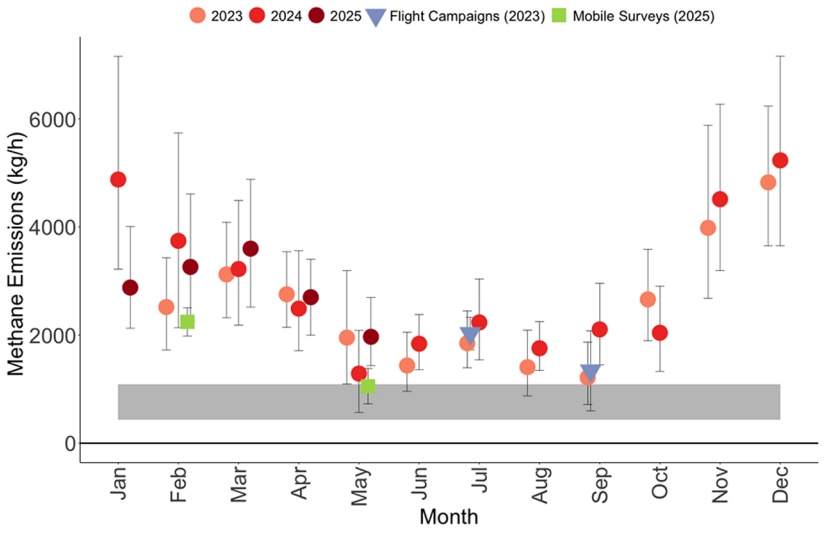

Figure 3. Monthly mean methane emissions estimated for the Middlesex County landfill complex (circles; light red for 2023, red for 2024, dark red for 2025), the flight campaigns (blue triangles), and the mobile estimates (green squares). The May 2025 mobile estimate is the mean of 2 days of measurements. Error bars represent the 95% confidence interval of the Monte Carlo-simulated emissions for that month. The range of values reported to the EPA GHGRP (429−1087 kg/h) for the entire landfill complex in 2023 (including both the WIP and captured methods) is shown as a shaded gray rectangle.

$$Q^{\text{tower}}_{(CH_4)} = \frac{\Sigma \Delta c_{\text{obs}}(wd)}{\Sigma \Delta c_{\text{GPD}}(wd)} \cdot Q^{\text{Initial}}_{CH_4} \quad (4)$$

For the mobile lab sampling, we integrated the observed and expected enhancements with respect to distance along the route and used the ratio to calculate the flux for that transect. This method has been shown elsewhere to perform better than alternative methods, such as using the peak height, inverting eq 3, or a line of best fit between the modeled and observed enhancements.[43,78] We adapted this method to estimate the flux for the stationary tower, using a Monte Carlo simulation to estimate the mean emission for each month. We drew 1000 random observed methane enhancements (c_{obs}) and predicted GPD enhancements (c_{GPD}, sampled with replacement) for each wind direction. We then used these 1000 simulated observation sets with eq 4 and calculated 1000 emissions estimates (Figure 2). We report the mean of these estimates as our estimate for a given month. As this method requires observations that cover the wind directions corresponding to the landfill and works best when averaging multiple data points for each wind direction, we include all observations from a given month for our draw of $\Delta c_{\text{obs}}(wd)$ and $\Delta c_{\text{GPD}}(wd)$ at each wind direction and estimate a single flux for that month.

We estimated the uncertainty of the monthly emissions from the 95% confidence interval of the Monte Carlo simulations. This does not account for any systematic uncertainty in the methodology, but does account for uncertainty in the meteorology and variability in emissions across the month. Using eq 3, we estimated that methane emissions of 50 kg/h produce enhancements of similar magnitude to the background variability observed at this site. Therefore, we estimated the limit of detection for our specific site, surrounding area, and instrumentation to be around 150 kg/h, assuming a 3σ limit of detection (Supporting Information S7).

While the tower method provides a more continuous record than sampling on individual days, it is not perfectly continuous. We only sampled the landfill complex during the approximately 20% of the deployment when winds were from the east. While there was not a significant difference in insolation or air temperature between easterly and westerly winds, times with easterly winds were slightly more likely to have decreasing pressure than times with westerly winds, with a mean pressure change of −0.2 hPa/h when winds were from the east.

As part of our mobile sampling, we identified small enhancements in microbial methane from the wastewater treatment plant to the east of the landfill, which, according to a high-resolution inventory from Pitt et al., is estimated to emit about 180 kg/h, far smaller than the observed emissions of methane from the landfill.[79] Seen from the stationary tower, this source would appear in the same wind direction as the landfill, but mobile sampling with winds from another directions allowed us to separate the various methane sources. The observed methane fluxes were below 200 kg/h using the GPD method and thus likely had very little effect on the estimated emission for the landfill at the tower. We also attempted to quantify methane emissions from the composting facility to the north of the landfill and estimated an upper bound of emissions at 150 kg/h.

Emissions Drivers

To test the effect of different drivers on methane emissions, we calculated a single flux (covering multiple years) for variables of interest, such as the air temperature or the change in atmospheric pressure over the preceding 6 h. For example, we selected the observed methane enhancements and predicted $\Delta c(x,y,z)$ from eq 3 for all times when the air temperature was between 15 and 16 °C. We then, following eq 4, binned the data by wind direction, and calculated the ratio of sum of the observed enhancements to the sum of the predicted enhancements in 1000 Monte Carlo draws of the observed and modeled enhancements at each wind direction. We report the mean of these 1000 simulations as a single flux estimate for all of the data with a given temperature. This required grouping data from multiple years to provide enough data to calculate a flux for the variable of interest. While we expect that methane emissions changed from year to year as the landfill grew and aged, the magnitude of these changes was likely far smaller

https://doi.org/10.1021/acs.est.5c16757
Environ. Sci. Technol. XXXX, XXX, XXX−XXX

than the variability within a given month or temperature range and we do not expect the annual trend to significantly effect our results.

We calculated a flux for temperature or pressure bins that included observations in at least 70 of the 1° wind direction bins within 45° of the center of the plume, which typically required around 1000 30-s intervals to fulfill. To have enough data in each bin, the highest and lowest bin contain all data above or below that threshold (e.g., all temperatures below −3 °C) were binned together. The temperature ranges are not evenly spaced to ensure sufficient wind direction coverage within each range.

RESULTS AND DISCUSSION

The tower was downwind of the landfill during approximately 20% of the deployment, providing semicontinuous measurements that allow us to assess the variability of methane emissions and decrease the likelihood of sampling bias in the results. We observed a strong seasonality in methane emissions, with a peak in the winter and a minimum in the summer, driven by a strong dependence on the change in atmospheric pressure and air temperature (Figures 3−5). Methane emissions were largest when pressure was declining quickly or when air temperatures were below 0 °C. The yearly mean estimate of methane emissions from the tower method was 2700 ± 300 kg/h in 2023 and 2,900 ± 400 kg/h in 2024. The flight campaigns estimated methane emissions at 2000 ± 300 and 1300 ± 700 kg/h for STAQS and MethaneAIR, respectively, in summer 2023. Work elsewhere has shown that active airborne methods, such as the HALO used on STAQS, and passive airborne methods, used for MethaneAIR, agree within 13%, indicating that the difference between the airborne estimates is not solely methodological.[47]

Seasonality of Methane Emissions

In each year, we observed a consistent cycle with a maximum of methane emissions in the winter and a minimum in the summer, a pattern that is consistent with other landfills in similar climates.[22,29,30] There is strong agreement between the magnitude of emissions from the tower method and the established mobile and aircraft methods (Figure 3). The tower method reduces potential sampling bias and provides more robust estimates of total monthly methane emissions, rather than snapshots in time from individual days of mobile or chamber measurements.

Emissions Drivers

Two commonly identified drivers of methane emissions are changes in atmospheric pressure and temperature-driven methane oxidation, both of which impact emissions here. Decreasing pressure allows methane produced inside the landfill to escape into the atmosphere. Previous work found that the slope of the 6-h atmospheric pressure change (referred to as the 6-h slope) was the best predictor of pressure-based methane emissions.[16−19] We observed that methane emissions leveled off below a 6-h slope of −1 hPa/h and were not a clear function of pressure change for 6-h slopes below this threshold (Figure 4). This threshold is comparable to around −1 hPa/h at an open landfill and −1.5 hPa/h at a closed landfill in Denmark.[18−20] We also observed methane emissions that were not significantly different from 0 when the slope of the pressure change was above 0.75 hP/h, while work at the closed Danish landfill found emissions near 0 at about 0.25 hPa/h. Methane emissions at open-faced landfills have a lower barrier to escape

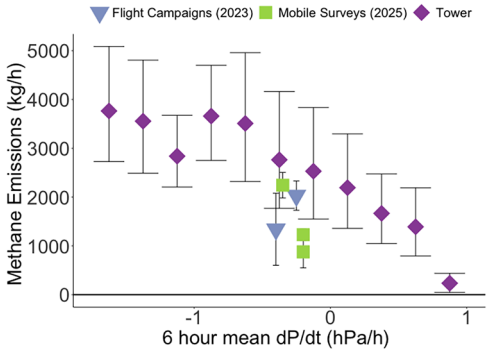

Figure 4. Mean estimated methane emissions from the tower (purple diamonds) binned by 6-h mean pressure change at the landfill. The x-coordinate represents the midpoint of the range (i.e., the point at −0.125 hPa/h includes all data between −0.25 and 0 hPa/h). Results from the aircraft (blue triangles) and drives (green squares) are also shown.

into the atmosphere than at closed faces due to the smaller, less compact cover layer. This may allow more methane to escape at smaller pressure declines or even as pressure increases at open-faced landfills. Gillespie et al. found a linear relationship with pressure change over a significantly larger range of pressure changes, with methane emissions only reaching 0 around 3 hPa/h for pressure change estimated over a 19-h window rather than 6-h.[29] Our results generally agree with Gillespie et al. (2024) and the results from Denmark despite three distinct measurement strategies. Gillespie et al. (2024) and estimates from the Danish landfill see a larger range of pressure changes but have fewer data points in each pressure bin. We have two and a half years of observations, which ensures that each pressure bin has sufficient data to minimize the impact of other drivers.

Temperature affects methane emissions through changes in the rates of methane production within the landfill and methane oxidation in the cover soil. Oxidation occurs in the top 40 cm of soil, where available oxygen allows methanotrophs to grow and remove methane, while methane production occurs deeper in the landfill.[11] The optimal temperature for both processes is around 30 °C.[11] However, the soil near the surface exhibits much larger seasonal temperature changes than in the interior of the landfill, which is insulated from the air. In temperate climates where air temperatures in the winter fall below freezing, methane emissions are typically highest during the winter.[23−25,35] This has been observed at open and closed landfills with modern management.[22,27,29,30] In warm, arid climates, studies have found the opposite trend, with open and closed landfills both emitting more methane during the summer.[28,80−82] Studies of California landfills form the basis for models of methane emissions used by the US Department of Agriculture, but warm, arid climates may not represent all landfills in the US.[83]

Our observed trend of methane emissions with temperature matches previous results in colder climates. Czepiel et al. found no relationship between temperature and methane emissions at high temperatures but a strong negative relationship overall.[14] We observed this same trend, as methane emissions did not change with temperature above 15 °C but increased with decreasing temperature below 15 °C (Figure 5). At low temperatures, Maurice et al. found that temperatures below 0 °C are associated with sharp increases in methane emissions due to soil freezing.[26] This contrasts with the results of

https://doi.org/10.1021/acs.est.5c16757
Environ. Sci. Technol. XXXX, XXX, XXX−XXX

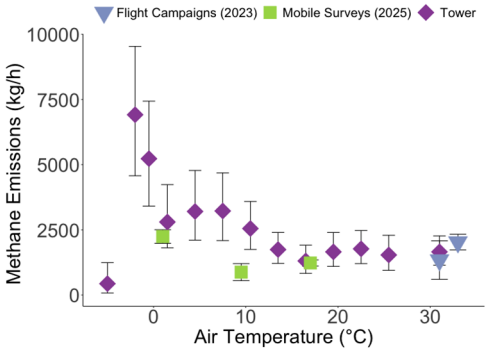

Figure 5. Mean estimated methane emissions from the tower (purple diamonds) binned by air temperature at the landfill. Results from the aircraft (blue triangles) and drives (green squares) are also shown.

Gillespie et al., who found that methane emissions decreased for air temperatures below 0 °C.[29] Our results indicate that methane emissions increased by over 50% for air temperatures between −3 and 0 °C relative to emissions for air temperatures between 0 and 3 °C. However, methane emissions when the air temperature was below −3 °C were the lowest of any bin.

Comparison of Methods

Methane emissions calculated using the tower, mobile, and aircraft methods show good agreement, but the semi-continuous tower method adds important context of seasonality and pressure dependence. In months with aircraft observations, we observed similar methane emissions for the month at the tower as observed by the aircraft. However, our aircraft measurements cannot reproduce the seasonality with just two observations, potentially leading to biased methane emissions estimates. Aircraft campaigns, by their nature, make limited numbers of observations, typically within a small time window and often during the summer, when flying conditions are most favorable. Other papers based entirely on aircraft data have similar biases toward observations in the summer months (e.g., Cusworth et al.;[6] Scarpelli et al.[8]). Furthermore, aircraft, like satellites, typically cannot retrieve plumes through clouds. Since clouds are associated with low-pressure systems, aircraft and satellites may miss the highest methane emissions associated with low-pressure events. Aircraft and satellites therefore may not observe the largest methane emissions in the winter in cold climates and may underestimate yearly emissions everywhere due to the clear-sky bias.[39] This is reflected in our results, as the mean of the summertime aircraft estimates was 37% lower than the yearly tower-estimated methane emissions for 2023.

Our 2023 estimate of methane emissions (2700 ± 300 kg/h) is approximately 5 times greater (95% CI: 4.5, 5.5) than reported emissions to the EPA's GHGRP (536 kg/h). Cusworth et al. estimated a 170% underestimate of methane emissions across hundreds of landfills using aircraft measurements,[6] while Balasus et al. found a mean underestimate of 500% at four landfills in the southeastern US using four years of TROPOMI satellite observations.[10] Since landfills select which method to report to the GHGRP, this choice can influence the magnitude of the underestimate. We estimate the waste-in-place method underestimates methane emissions by 175% (95% CI: 144%, 203%), similar to the value in Cusworth et al. (2024).

POTENTIAL IMPACTS AND FUTURE WORK

The methane emission rate from the NYC metro area has been estimated at 33,000 and 37,000 kg/h based on tower network observations in January to June of 2023 and 2024.[84] The Middlesex landfill complex therefore accounts for approximately 8% of methane emissions in the NYC metro area in the first half of both 2023 and 2024. Other work prior to 2023 found similar estimates for methane emissions in the entire NYC metro area.[7,79,85−87] If Middlesex landfill emitted a similar amount of methane from 2018 to 2022, it would account for 7−9% of emissions in those years as well.

Our results provide insight into potential strategies for reducing landfill methane emissions. Operators may be able to design strategies to maximize the efficiency of active gas capture during times when methane emissions are largest, such as for very low temperatures or immediately preceding low pressure events. Leak detection should be scheduled for times when the pressure is declining or days below freezing to best identify and mitigate emission hotspots. Operators of open landfills could also add additional daily soil cover during the winter or when low pressure systems are in the forecast.

Our results are also relevant to the design of future airborne and mobile drive measurement campaigns. Current inventories indicate that landfills emit an estimated 17% of anthropogenic methane emissions in the US, though results from satellites and aircraft campaigns indicate that this is an underestimate. Our results emphasize the importance of observing methane throughout the seasonal cycle. Aircraft campaigns and satellites cannot measure through clouds, which are more common on low-pressure days, and aircraft campaigns often occur during the summer months, rather than capturing the full seasonal cycle of methane emissions. The aircraft campaigns at this landfill complex underestimated year-round methane emissions by 37% relative to the tower-based emissions due to the observed seasonal trends. Therefore, estimates of sector-wide methane emissions based on aircraft and satellite measurements may underestimate emissions. Ground-based measurements without a clear sampling bias can help improve overall estimates of methane emissions.

Long-term measurements of methane emissions allow policymakers to target climate mitigation efforts and track the efficacy of these policies. Active landfills, with their large but uncertain methane emissions, are a perfect target for long-term measurements. The tower methodology developed here could be applied to other sites effectively with a few considerations. First, these sites must have a point source emission much larger than emissions from all sources in the surrounding area. Large landfills, which in the US are often located in rural areas, may fit this description, but areas with many nearby point sources likely would not. In this case, mobile surveys should be conducted around the landfill to quantify any other potential methane sources. Second, the method relies on a reasonable estimate of the background methane upwind of the point source. The best method would involve measurement sites on two opposite sides of the point source. If this is not possible, confirming that the background upwind of the point source matches the tower observations from a different wind direction can be done with mobile measurements. Third, methane observations must be far enough away (typically at least 2−3 km) from the point source for the Gaussian plume approximation to hold.

https://doi.org/10.1021/acs.est.5c16757
Environ. Sci. Technol. XXXX, XXX, XXX−XXX

■ ASSOCIATED CONTENT

Data Availability Statement

Associated data can be found at 10.5061/dryad.ghx3ffc34.

Supporting Information

The Supporting Information is available free of charge at https://pubs.acs.org/doi/10.1021/acs.est.5c16757.

Additional materials regarding methods, results, and discussion (PDF)

■ AUTHOR INFORMATION

Corresponding Author

Andrew Hallward-Driemeier − *Department of Earth and Environmental Sciences, Columbia University, New York, New York 10027, United States;* orcid.org/0000-0003-1125-288X; Email: ah3956@columbia.edu

Authors

Yuwei Zhao − *Department of Earth and Environmental Sciences, Columbia University, New York, New York 10027, United States;* orcid.org/0000-0002-6104-8337

Matthew Drews − *Office of Climate Action, Rutgers University, New Brunswick, New Jersey 08901, United States*

Maryann Sargent − *Department of Earth and Planetary Sciences, Harvard University, Cambridge, Massachusetts 02138, United States*

Steven Wofsy − *Department of Earth and Planetary Sciences, Harvard University, Cambridge, Massachusetts 02138, United States*

Rory Barton-Grimley − *NASA Langley Research Center, Hampton, Virginia 23666, United States*

Ashwin Yerasi − *Analytical Mechanics Associates, Inc., Hampton, Virginia 23666, United States*

James Collins − *Coherent Applications, Inc., Hampton, Virginia 23666, United States*

Amin Nehrir − *NASA Langley Research Center, Hampton, Virginia 23666, United States*

Róisín Commane − *Department of Earth and Environmental Sciences, Columbia University, New York, New York 10027, United States; Lamont-Doherty Earth Observatory, Columbia University, Palisades, New York 10964, United States;* orcid.org/0000-0003-1373-1550

Complete contact information is available at: https://pubs.acs.org/10.1021/acs.est.5c16757

Notes

The authors declare no competing financial interest.

■ ACKNOWLEDGMENTS

The authors would like to thank New York State Energy Research Development Agency for supporting this work (contract #183867). We would also like to thank NASA Earth Science Division Research and Analysis for funding the STAQS campaign and the Environmental Defense Fund and Harvard University for funding MethaneAIR. We would also like to thank Greg Stey (Westchester County) and Michael Flaherty (Nassau County) for support and Mathieu Gerbush and David Robinson (Office of the New Jersey State Climatologist) for sharing data.

■ REFERENCES

(1) Forster, P.; Storelvmo, T.; Armour, K.; Collins, W.; Dufresne, J.-L.; Frame, D.; Lunt, D.; Mauritsen, T.; Palmer, M.; Watanabe, M.; Wild, M.; Zhang, H. *Climate Change 2021 − The Physical Science Basis: Working Group I Contribution to the Sixth Assessment Report of the Intergovernmental Panel on Climate Change*, 1st ed.; Cambridge University Press, 2023; pp 923−1054.

(2) Jones, M. W.; Peters, G. P.; Gasser, T.; Andrew, R. M.; Schwingshackl, C.; Gütschow, J.; Houghton, R. A.; Friedlingstein, P.; Pongratz, J.; Le Quéré, C. National contributions to climate change due to historical emissions of carbon dioxide, methane, and nitrous oxide since 1850. *Sci. Data* **2023**, *10*, No. 155.

(3) Canadell, J.; Monteiro, P.; Costa, M.; da Cunha, L. C.; Cox, P.; Eliseev, A.; Henson, S.; Ishii, M.; Jaccard, S.; Koven, C.; Lohila, A.; Patra, P.; Piao, S.; Rogelj, J.; Syampungani, S.; Zaehle, S.; Zickfeld, K. *Climate Change 2021 - The Physical Science Basis: Working Group I Contribution to the Sixth Assessment Report of the Intergovernmental Panel on Climate Change*, 1st ed.; Cambridge University Press, 2023; pp; pp 673−816.

(4) EPA. *Inventory of U.S. Greenhouse Gas Emissions and Sinks*, 20241990-2022.

(5) Lu, X.; Jacob, D. J.; Wang, H.; Maasakkers, J. D.; Zhang, Y.; Scarpelli, T. R.; Shen, L.; Qu, Z.; Sulprizio, M. P.; Nesser, H.; Bloom, A. A.; Ma, S.; Worden, J. R.; Fan, S.; Parker, R. J.; Boesch, H.; Gautam, R.; Gordon, D.; Moran, M. D.; Reuland, F.; Villasana, C. A. O.; Andrews, A. Methane emissions in the United States, Canada, and Mexico: evaluation of national methane emission inventories and 2010−2017 sectoral trends by inverse analysis of in situ (GLOBALVIEWplus CH_4 ObsPack) and satellite (GOSAT) atmospheric observations. *Atmos. Chem. Phys.* **2022**, *22*, 395−418.

(6) Cusworth, D. H.; Duren, R. M.; Ayasse, A. K.; Jiorle, R.; Howell, K.; Aubrey, A.; Green, R. O.; Eastwood, M. L.; Chapman, J. W.; Thorpe, A. K.; Heckler, J.; Asner, G. P.; Smith, M. L.; Thoma, E.; Krause, M. J.; Heins, D.; Thorneloe, S. Quantifying methane emissions from United States landfills. *Science* **2024**, *383*, 1499−1504.

(7) Nesser, H.; Jacob, D. J.; Maasakkers, J. D.; Lorente, A.; Chen, Z.; Lu, X.; Shen, L.; Qu, Z.; Sulprizio, M. P.; Winter, M.; Ma, S.; Bloom, A. A.; Worden, J. R.; Stavins, R. N.; Randles, C. A. High-resolution US methane emissions inferred from an inversion of 2019 TROPOMI satellite data: contributions from individual states, urban areas, and landfills. *Atmos. Chem. Phys.* **2024**, *24*, 5069−5091.

(8) Scarpelli, T. R.; Cusworth, D. H.; Duren, R. M.; Kim, J.; Heckler, J.; Asner, G. P.; Thoma, E.; Krause, M. J.; Heins, D.; Thorneloe, S. Investigating Major Sources of Methane Emissions at US Landfills. *Environ. Sci. Technol.* **2024**, *58*, 21545−21556, DOI: 10.1021/acs.est.4c07572.

(9) Wang, X.; Jacob, D. J.; Nesser, H.; Balasus, N.; Estrada, L. A.; Sulprizio, M. P.; Cusworth, D. H.; Scarpelli, T. R.; Chen, Z.; East, J. D.; Varon, D. J. Quantifying urban and landfill methane emissions in the United States using TROPOMI satellite data. *Sci. Adv.* **2026**, *12*, No. eadz9308.

(10) Balasus, N.; Jacob, D. J.; Maxemin, G.; Jenks, C.; Nesser, H.; Maasakkers, J. D.; Cusworth, D. H.; Scarpelli, T. R.; Varon, D. J.; Wang, X. Satellite monitoring of annual US landfill methane emissions and trends. *Environ. Res. Lett.* **2025**, *20*, No. 024007.

(11) Scheutz, C.; Kjeldsen, P.; Bogner, J. E.; De Visscher, A.; Gebert, J.; Hilger, H. A.; Huber-Humer, M.; Spokas, K. Microbial methane oxidation processes and technologies for mitigation of landfill gas emissions. *Waste Manage. Res.* **2009**, *27*, 409−455.

(12) Delkash, M.; Zhou, B.; Han, B.; Chow, F. K.; Rella, C. W.; Imhoff, P. T. Short-term landfill methane emissions dependency on wind. *Waste Manage.* **2016**, *55*, 288−298.

(13) Poulsen, T. G.; Christophersen, M.; Moldrup, P.; Kjeldsen, P. Relating landfill gas emissions to atmospheric pressure using numerical modelling and state-space analysis. *Waste Manage. Res.* **2003**, *21*, 356−366.

(14) Czepiel, P.; Shorter, J.; Mosher, B.; Allwine, E.; McManus, J.; Harriss, R.; Kolb, C.; Lamb, B. The influence of atmospheric pressure on landfill methane emissions. *Waste Manage.* **2003**, *23*, 593−598.

(15) Gebert, J.; Groengroeft, A. Passive landfill gas emission - Influence of atmospheric pressure and implications for the operation of methane-oxidising biofilters. *Waste Manage.* **2006**, *26*, 245−251.
(16) Xu, L.; Lin, X.; Amen, J.; Welding, K.; McDermitt, D. Impact of changes in barometric pressure on landfill methane emission. *Global Biogeochem. Cycles* **2014**, *28*, 679−695.
(17) Delkash, M.; Chow, F. K.; Imhoff, P. T. Diurnal landfill methane flux patterns across different seasons at a landfill in Southeastern US. *Waste Manage.* **2022**, *144*, 76−86.
(18) Kissas, K.; Ibrom, A.; Kjeldsen, P.; Scheutz, C. Methane emission dynamics from a Danish landfill: The effect of changes in barometric pressure. *Waste Manage.* **2022**, *138*, 234−242.
(19) Kissas, K.; Ibrom, A.; Kjeldsen, P.; Scheutz, C. Annual upscaling of methane emission field measurements from two Danish landfills, using empirical emission models. *Waste Manage.* **2022**, *150*, 191−201.
(20) Kissas, K.; Kjeldsen, P.; Ibrom, A.; Scheutz, C. The effect of barometric pressure changes on the performance of a passive biocover system, Skellingsted landfill, Denmark. *Waste Manage.* **2023**, *156*, 216−226.
(21) Perdikea, K.; Mehrotra, A. K.; Hettiaratchi, J. P. A. Study of thin biocovers (TBC) for oxidizing uncaptured methane emissions in bioreactor landfills. *Waste Manage.* **2008**, *28*, 1364−1374.
(22) Rachor, I. M.; Gebert, J.; Gröngröft, A.; Pfeiffer, E. Variability of methane emissions from an old landfill over different time-scales. *Eur. J. Soil Sci.* **2013**, *64*, 16−26.
(23) Czepiel, P. M.; Mosher, B.; Crill, P. M.; Harriss, R. C. Quantifying the effect of oxidation on landfill methane emissions. *J. Geophys. Res.: Atmos.* **1996**, *101*, 16721−16729.
(24) Börjesson, G.; Svensson, B. H. Seasonal and Diurnal Methane Emissions From a Landfill and Their Regulation By Methane Oxidation. *Waste Manage. Res.* **1997**, *15*, 33−54.
(25) Chanton, J.; Liptay, K. Seasonal variation in methane oxidation in a landfill cover soil as determined by an in situ stable isotope technique. *Global Biogeochem. Cycles* **2000**, *14*, 51−60.
(26) Maurice, C.; Lagerkvist, A. LFG emission measurements in cold climatic conditions: seasonal variations and methane emissions mitigation. *Cold Reg. Sci. Technol.* **2003**, *36*, 37−46.
(27) Tecle, D.; Lee, J.; Hasan, S. Quantitative analysis of physical and geotechnical factors affecting methane emission in municipal solid waste landfill. *Environ. Geol.* **2009**, *56*, 1135−1143.
(28) Spokas, K.; Bogner, J.; Corcoran, M.; Walker, S. From California dreaming to California data: Challenging historic models for landfill CH4 emissions. *Elementa: Sci. Anthropocene* **2015**, *3*, No. 000051.
(29) Gillespie, L. D.; Ars, S.; Alkadri, S.; Urya, S.; Khoo, T.; Fraser, S.; Vogel, F.; Wunch, D. Estimating methane emissions from the waste sector in southern ontario using atmospheric measurements. *J. Air Waste Manage. Assoc.* **2024**, *75*, 144−163, DOI: 10.1080/10962247.2024.2435340.
(30) Li, H.; Meng, B.; Yue, B.; Gao, Q.; Ma, Z.; Zhang, W.; Li, T.; Yu, L. Seasonal CH4 and CO2 effluxes in a final covered landfill site in Beijing, China. *Sci. Total Environ.* **2020**, *725*, No. 138355.
(31) Goldsmith, C. D.; Chanton, J.; Abichou, T.; Swan, N.; Green, R.; Hater, G. Methane emissions from 20 landfills across the United States using vertical radial plume mapping. *J. Air Waste Manage. Assoc.* **2012**, *62*, 183−197.
(32) Cambaliza, M. O. L.; Bogner, J. E.; Green, R. B.; Shepson, P. B.; Harvey, T. A.; Spokas, K. A.; Stirm, B. H.; Corcoran, M. Field measurements and modeling to resolve m2 to km2 CH4 emissions for a complex urban source: An Indiana landfill study. *Elementa: Sci. Anthropocene* **2017**, *5*, No. 36.
(33) Olaguer, E.; Jeltema, S.; Gauthier, T.; Jermalowicz, D.; Ostaszewski, A.; Batterman, S.; Xia, T.; Raneses, J.; Kovalchick, M.; Miller, S.; Acevedo, J.; Lamb, J.; Benya, J.; Wendling, A.; Zhu, J. Landfill Emissions of Methane Inferred from Unmanned Aerial Vehicle and Mobile Ground Measurements. *Atmosphere* **2022**, *13*, No. 983.
(34) Omidi, A.; Bourlon, E.; Khaleghi, A.; Tarakki, N.; Martino, R.; Stuart, J.; Risk, D. Most landfill methane emissions Escape detection in EPA21 surface emission monitoring surveys. *Waste Manage.* **2025**, *207*, No. 115104.
(35) Christophersen, M.; Kjeldsen, P.; Holst, H.; Chanton, J. Lateral gas transport in soil adjacent to an old landfill: factors governing emissions and methane oxidation. *Waste Manage. Res.* **2001**, *19*, 595−612.
(36) Spokas, K.; Bogner, J.; Chanton, J.; Morcet, M.; Aran, C.; Graff, C.; Golvan, Y. M.-L.; Hebe, I. Methane mass balance at three landfill sites: What is the efficiency of capture by gas collection systems? *Waste Manage.* **2006**, *26*, 516−525.
(37) Riddick, S. N.; Ancona, R.; Cheptonui, F.; Bell, C. S.; Duggan, A.; Bennett, K. E.; Zimmerle, D. J. A cautionary report of calculating methane emissions using low-cost fence-line sensors. *Elementa: Sci. Anthropocene* **2022**, *10*, No. 00021.
(38) Zhu, H.; Letzel, M. O.; Reiser, M.; Kranert, M.; Bächlin, W.; Flassak, T. A new approach to estimation of methane emission rates from landfills. *Waste Manage.* **2013**, *33*, 2713−2719.
(39) Gillespie, L. D.; Ars, S.; Worthy, C.; Brantley, H.; Green, R.; Scarpelli, T. R.; Cusworth, D. H.; Vogel, F.; Wunch, D. Comparison of Landfill Methane Emission Quantification Using Multiple Observation Methods. *ACS ES&T Air* **2025**, *2*, 2786−2798, DOI: 10.1021/acsestair.5c00127.
(40) Babilotte, A.; Lagier, T.; Fiani, E.; Taramini, V. Fugitive Methane Emissions from Landfills: Field Comparison of Five Methods on a French Landfill. *J. Environ. Eng.* **2010**, *136*, 777−784.
(41) Abichou, T.; Clark, J.; Tan, S.; Chanton, J.; Hater, G.; Green, R.; Goldsmith, D.; Barlaz, M. A.; Swan, N. Uncertainties Associated with the Use of Optical Remote Sensing Technique to Estimate Surface Emissions in Landfill Applications. *J. Air Waste Manage. Assoc.* **2010**, *60*, 460−470.
(42) Foster-Wittig, T. A.; Thoma, E. D.; Green, R. B.; Hater, G. R.; Swan, N. D.; Chanton, J. P. Development of a mobile tracer correlation method for assessment of air emissions from landfills and other area sources. *Atmos. Environ.* **2015**, *102*, 323−330.
(43) Mønster, J. G.; Samuelsson, J.; Kjeldsen, P.; Rella, C. W.; Scheutz, C. Quantifying methane emission from fugitive sources by combining tracer release and downwind measurements - A sensitivity analysis based on multiple field surveys. *Waste Manage.* **2014**, *34*, 1416−1428.
(44) Shaw, J. T.; Shah, A.; Yong, H.; Allen, G. Methods for quantifying methane emissions using unmanned aerial vehicles: a review. *Philos. Trans. R. Soc., A* **2021**, *379*, No. 20200450.
(45) Kumar, P.; Caldow, C.; Broquet, G.; Shah, A.; Laurent, O.; Yver-Kwok, C.; Ars, S.; Defratyka, S.; Gichuki, S. W.; Lienhardt, L.; Lozano, M.; Paris, J.-D.; Vogel, F.; Bouchet, C.; Allegrini, E.; Kelly, R.; Juery, C.; Ciais, P. Detection and long-term quantification of methane emissions from an active landfill. *Atmos. Meas. Tech.* **2024**, *17*, 1229−1250.
(46) Duren, R. M.; Thorpe, A. K.; Foster, K. T.; Rafiq, T.; Hopkins, F. M.; Yadav, V.; Bue, B. D.; Thompson, D. R.; Conley, S.; Colombi, N. K.; Frankenberg, C.; McCubbin, I. B.; Eastwood, M. L.; Falk, M.; Herner, J. D.; Croes, B. E.; Green, R. O.; Miller, C. E. California's methane super-emitters. *Nature* **2019**, *575*, 180−184.
(47) Krautwurst, S.; Fruck, C.; Wolff, S.; Borchardt, J.; Huhs, O.; Gerilowski, K.; Gałkowski, M.; Kiemle, C.; Quatrevalet, M.; Wirth, M.; Mallaun, C.; Burrows, J. P.; Gerbig, C.; Fix, A.; Bösch, H.; Bovensmann, H. Identification and quantification of CH_4 emissions from Madrid landfills using airborne imaging spectrometry and greenhouse gas lidar. *Atmos. Chem. Phys.* **2025**, *25*, 14669−14702.
(48) Zhang, S.; Lei, M.; Huang, X.; Zhang, Y. Evaluation of methane emission from MSW landfills in China, India, and the U.S. from space using a two-tier approach. *J. Environ. Manage.* **2025**, *377*, No. 124705.
(49) Bai, S.; Li, F.; Yan, Y.; Huang, Q.; Jiang, F.; Chen, H.; Zhang, Y. Seasonal Variations of Methane Emissions From a Urumqi Landfill in China and Its Driving Factors Using Hyperspectral Satellite Time-Series Observations. *J. Geophys. Res.: Atmos.* **2025**, *130*, No. e2025JD044272.

(50) Dogniaux, M.; Maasakkers, J. D.; Girard, M.; Jervis, D.; McKeever, J.; Schuit, B. J.; Sharma, S.; Lopez-Noreña, A.; Varon, D. J.; Aben, I. Global satellite survey reveals uncertainty in landfill methane emissions. *Nature* **2025**, *647*, 397−402, DOI: 10.1038/s41586-025-09683-8.
(51) Giani, L.; Bredenkamp, J.; Eden, I. Temporal and spatial variability of the CH4 dynamics of landfill cover soils. *J. Plant Nutr. Soil Sci.* **2002**, *165*, 205−210.
(52) Ute-Röwer, I.; Streese-Kleeberg, J.; Scharff, H.; Pfeiffer, E.-M.; Gebert, J. Optimized Landfill Biocover for CH4 Oxidation II: Implications of Spatially Heterogeneous Fluxes for Monitoring and Emission Prediction. *Curr. Environ. Eng.* **2016**, *3*, 94−106.
(53) Yeşiller, N.; Hanson, J. L.; Manheim, D. C.; Newman, S.; Guha, A. Assessment of methane emissions from a California landfill using concurrent experimental, inventory, and modeling approaches. *Waste Manage.* **2022**, *154*, 146−159.
(54) Mønster, J.; Kjeldsen, P.; Scheutz, C. Methodologies for measuring fugitive methane emissions from landfills - A review. *Waste Manage.* **2019**, *87*, 835−859.
(55) U.S. Environmental Protection Agency Office of Atmospheric Protection Greenhouse Gas Reporting Program (GHGRP). www.epa.gov/ghgreporting.
(56) Drews, M. P. The modernization of the Rutgers Photochemical Assessment Monitoring Site and analysis of its multi-decadal boundary layer wind record, M.Sc. thesis; Rutgers University2024.
(57) Commane, R.; Hallward-Driemeier, A.; Murray, L. T. Intercomparison of commercial analyzers for atmospheric ethane and methane observations. *Atmos. Meas. Tech.* **2023**, *16*, 1431−1441.
(58) Drusch, M.; Del Bello, U.; Carlier, S.; Colin, O.; Fernandez, V.; Gascon, F.; Hoersch, B.; Isola, C.; Laberinti, P.; Martimort, P.; Meygret, A.; Spoto, F.; Sy, O.; Marchese, F.; Bargellini, P. Sentinel-2: ESA's Optical High-Resolution Mission for GMES Operational Services. *Remote Sens. Environ.* **2012**, *120*, 25−36.
(59) Moore, D. P.; Li, N. P.; Wendt, L. P.; Castañeda, S. R.; Falinski, M. M.; Zhu, J.-J.; Song, C.; Ren, Z. J.; Zondlo, M. A. Underestimation of Sector-Wide Methane Emissions from United States Wastewater Treatment. *Environ. Sci. Technol.* **2023**, *57*, 4082−4090.
(60) Caulton, D. R.; Li, Q.; Bou-Zeid, E.; Fitts, J. P.; Golston, L. M.; Pan, D.; Lu, J.; Lane, H. M.; Buchholz, B.; Guo, X.; McSpiritt, J.; Wendt, L.; Zondlo, M. A. Quantifying uncertainties from mobile-laboratory-derived emissions of well pads using inverse Gaussian methods. *Atmos. Chem. Phys.* **2018**, *18*, 15145−15168.
(61) Nehrir, A. R.; Hair, J. W.; Ferrare, R. A.; Hostetler, C. A.; Kooi, S. A.; Notari, A. The High Altitude Lidar Observatory (HALO): a multi-function lidar and technology testbed for airborne and space-based measurements of water vapor and methane 2018 https://esto.nasa.gov/forums/estf2018/presentations/Nehrir_ESTF2018_A1P2.pdf.
(62) Barton-Grimley, R. A.; Nehrir, A. R.; Kooi, S. A.; Collins, J. E.; Harper, D. B.; Notari, A.; Lee, J.; DiGangi, J. P.; Choi, Y.; Davis, K. J. Evaluation of the High Altitude Lidar Observatory (HALO) methane retrievals during the summer 2019 ACT-America campaign. *Atmos. Meas. Tech.* **2022**, *15*, 4623−4650.
(63) Hair, J. W.; Hostetler, C. A.; Cook, A. L.; Harper, D. B.; Ferrare, R. A.; Mack, T. L.; Welch, W.; Izquierdo, L. R.; Hovis, F. E. Airborne High Spectral Resolution Lidar for profiling aerosol optical properties. *Appl. Opt.* **2008**, *47*, 6734−6752.
(64) Scarino, A. J.; Obland, M. D.; Fast, J. D.; Burton, S. P.; Ferrare, R. A.; Hostetler, C. A.; Berg, L. K.; Lefer, B.; Haman, C.; Hair, J. W.; Rogers, R. R.; Butler, C.; Cook, A. L.; Harper, D. B. Comparison of mixed layer heights from airborne high spectral resolution lidar, ground-based measurements, and the WRF-Chem model during CalNex and CARES. *Atmos. Chem. Phys.* **2014**, *14*, 5547−5560.
(65) Judd, L.; Sullivan, J.; Crawford, J.; Lefer, B.; Yang Margin, M.; Travies, K.; Chance, K.; Liu, X.; Janz, S.; Hair, J.; Shingler, T.; Nehrir, A.; Barton-Grimley, R.; Green, R.; Eastwood, M.; Hanisco, T.; McDonald, B.; Warneke, C.; Schwantes, B.; Mak, J.; Valin, L.; Demetillo, A.; Team, S. Accelerating TEMPO Air Quality Science Through STAQS 2022 https://ntrs.nasa.gov/api/citations/20220018296/downloads/STAQS_AGU_Poster_v3.pdf.
(66) Chulakadabba, A.; Sargent, M.; Lauvaux, T.; Benmergui, J. S.; Franklin, J. E.; Chan Miller, C.; Wilzewski, J. S.; Roche, S.; Conway, E.; Souri, A. H.; Sun, K.; Luo, B.; Hawthrone, J.; Samra, J.; Daube, B. C.; Liu, X.; Chance, K.; Li, Y.; Gautam, R.; Omara, M.; Rutherford, J. S.; Sherwin, E. D.; Brandt, A.; Wofsy, S. C. Methane point source quantification using MethaneAIR: a new airborne imaging spectrometer. Atmospheric. *Meas. Tech.* **2023**, *16*, 5771−5785.
(67) Conway, E. K.; Souri, A. H.; Benmergui, J.; Sun, K.; Liu, X.; Staebell, C.; Chan Miller, C.; Franklin, J.; Samra, J.; Wilzewski, J.; Roche, S.; Luo, B.; Chulakadabba, A.; Sargent, M.; Hohl, J.; Daube, B.; Gordon, I.; Chance, K.; Wofsy, S. Level0 to Level1B processor for MethaneAIR. Atmospheric. *Meas. Tech.* **2024**, *17*, 1347−1362.
(68) Staebell, C.; Sun, K.; Samra, J.; Franklin, J.; Chan Miller, C.; Liu, X.; Conway, E.; Chance, K.; Milligan, S.; Wofsy, S. Spectral calibration of the MethaneAIR instrument. Atmospheric. *Meas. Tech.* **2021**, *14*, 3737−3753.
(69) Chan Miller, C.; Roche, S.; Wilzewski, J. S.; Liu, X.; Chance, K.; Souri, A. H.; Conway, E.; Luo, B.; Samra, J.; Hawthorne, J.; Sun, K.; Staebell, C.; Chulakadabba, A.; Sargent, M.; Benmergui, J. S.; Franklin, J. E.; Daube, B. C.; Li, Y.; Laughner, J. L.; Baier, B. C.; Gautam, R.; Omara, M.; Wofsy, S. C. Methane retrieval from MethaneAIR using the CO_2 proxy approach: a demonstration for the upcoming MethaneSAT mission. Atmospheric. *Meas. Tech.* **2024**, *17*, 5429−5454.
(70) Krings, T.; Gerilowski, K.; Buchwitz, M.; Hartmann, J.; Sachs, T.; Erzinger, J.; Burrows, J. P.; Bovensmann, H. Quantification of methane emission rates from coal mine ventilation shafts using airborne remote sensing data. *Atmos. Meas. Tech.* **2013**, *6*, 151−166.
(71) Amediek, A.; Ehret, G.; Fix, A.; Wirth, M.; Büdenbender, C.; Quatrevalet, M.; Kiemle, C.; Gerbig, C. CHARM-Fa new airborne integrated-path differential-absorption lidar for carbon dioxide and methane observations: measurement performance and quantification of strong point source emissions. *Appl. Opt.* **2017**, *56*, 5182−5197.
(72) Yang, S.; Talbot, R. W.; Frish, M. B.; Golston, L. M.; Aubut, N. F.; Zondlo, M. A.; Gretencord, C.; McSpiritt, J. Natural Gas Fugitive Leak Detection Using an Unmanned Aerial Vehicle: Measurement System Description and Mass Balance Approach. *Atmosphere* **2018**, *9*, No. 383.
(73) Varon, D. J.; Jacob, D. J.; McKeever, J.; Jervis, D.; Durak, B. O. A.; Xia, Y.; Huang, Y. Quantifying methane point sources from fine-scale satellite observations of atmospheric methane plumes. *Atmos. Meas. Tech.* **2018**, *11*, 5673−5686.
(74) Sadavarte, P.; Pandey, S.; Maasakkers, J. D.; Lorente, A.; Borsdorff, T.; Denier Van Der Gon, H.; Houweling, S.; Aben, I. Methane Emissions from Superemitting Coal Mines in Australia Quantified Using TROPOMI Satellite Observations. *Environ. Sci. Technol.* **2021**, *55*, 16573−16580.
(75) Dowell, D. C.; Alexander, C. R.; James, E. P.; Weygandt, S. S.; Benjamin, S. G.; Manikin, G. S.; Blake, B. T.; Brown, J. M.; Olson, J. B.; Hu, M.; Smirnova, T. G.; Ladwig, T.; Kenyon, J. S.; Ahmadov, R.; Turner, D. D.; Duda, J. D.; Alcott, T. I. The High-Resolution Rapid Refresh (HRRR): An Hourly Updating Convection-Allowing Forecast Model. Part I: Motivation and System Description. *Weather Forecast.* **2022**, *37*, 1371−1395.
(76) El Abbadi, S. H.; Feng, J.; Hodson, A. R.; Amouamouha, M.; Busse, M. M.; Polcuch, C.; Zhou, P.; Macknick, J.; Guest, J. S.; Stokes-Draut, J. R.; Dunn, J. B. Benchmarking greenhouse gas emissions from US wastewater treatment for targeted reduction. *Nat. Water* **2025**, *3*, 1133−1143.
(77) Stockie, J. M. The Mathematics of Atmospheric Dispersion Modeling. *SIAM Review* **2011**, *53*, 349−372.
(78) Albertson, J. D.; Harvey, T.; Foderaro, G.; Zhu, P.; Zhou, X.; Ferrari, S.; Amin, M. S.; Modrak, M.; Brantley, H.; Thoma, E. D. A Mobile Sensing Approach for Regional Surveillance of Fugitive Methane Emissions in Oil and Gas Production. *Environ. Sci. Technol.* **2016**, *50*, 2487−2497.

https://doi.org/10.1021/acs.est.5c16757
Environ. Sci. Technol. XXXX, XXX, XXX−XXX

(79) Pitt, J. R.; Lopez-Coto, I.; Karion, A.; Hajny, K. D.; Tomlin, J.; Kaeser, R.; Jayarathne, T.; Stirm, B. H.; Floerchinger, C. R.; Loughner, C. P.; Commane, R.; Gately, C. K.; Hutyra, L. R.; Gurney, K. R.; Roest, G. S.; Liang, J.; Gourdji, S.; Mueller, K. L.; Whetstone, J. R.; Shepson, P. B. Underestimation of Thermogenic Methane Emissions in New York City. *Environ. Sci. Technol.* **2024**, *58*, 9147−9157.
(80) Park, J.-W.; Shin, H.-C. Surface emission of landfill gas from solid waste landfill. *Atmos. Environ.* **2001**, *35*, 3445−3451.
(81) Gollapalli, M.; Kota, S. H. Methane emissions from a landfill in north-east India: Performance of various landfill gas emission models. *Environ. Pollut.* **2018**, *234*, 174−180.
(82) Bogner, J. E.; Spokas, K. A.; Chanton, J. P. Seasonal Greenhouse Gas Emissions (Methane, Carbon Dioxide, Nitrous Oxide) from Engineered Landfills: Daily, Intermediate, and Final California Cover Soils. *J. Environ. Qual.* **2011**, *40*, 1010−1020.
(83) Spokas, K.; Bogner, J.; Corcoran, M. Modeling landfill CH4 emissions. *Elementa: Sci. Anthropocene* **2021**, *9*, No. 00050.
(84) Schiferl, L. D.; Hallward-Driemeier, A.; Zhao, Y.; Toledo-Crow, R.; Commane, R. Missing wintertime methane emissions from New York City related to combustion. *Atmos. Chem. Phys.* **2025**, *25*, 15683−15700.
(85) Plant, G.; Kort, E. A.; Floerchinger, C.; Gvakharia, A.; Vimont, I.; Sweeney, C. Large Fugitive Methane Emissions From Urban Centers Along the U.S. East Coast. *Geophys. Res. Lett.* **2019**, *46*, 8500−8507.
(86) Plant, G.; Kort, E. A.; Brandt, A. R.; Chen, Y.; Fordice, G.; Gorchov Negron, A. M.; Schwietzke, S.; Smith, M.; Zavala-Araiza, D. Inefficient and unlit natural gas flares both emit large quantities of methane. *Science* **2022**, *377*, 1566−1571.
(87) Pitt, J. R.; Lopez-Coto, I.; Hajny, K. D.; Tomlin, J.; Kaeser, R.; Jayarathne, T.; Stirm, B. H.; Floerchinger, C. R.; Loughner, C. P.; Gately, C. K.; Hutyra, L. R.; Gurney, K. R.; Roest, G. S.; Liang, J.; Gourdji, S.; Karion, A.; Whetstone, J. R.; Shepson, P. B. New York City greenhouse gas emissions estimated with inverse modeling of aircraft measurements. *Elementa: Sci. Anthropocene* **2022**, *10*, No. 00082.

https://doi.org/10.1021/acs.est.5c16757
Environ. Sci. Technol. XXXX, XXX, XXX−XXX